Journal of ELECTRONIC MATERIALS, Vol. 44, No. 10, 2015
DOI: 10.1007/s11664-015-3845-y
© 2015 The Minerals, Metals & Materials Society

Numerical Examination of the Performance of a Thermoelectric Cooler with Peltier Heating and Cooling

CHANG NYUNG KIM[1,3] and JEONGHO KIM[2]

1.—Department of Mechanical Engineering, College of Engineering, Kyung Hee University, Yong-in, Kyunggi-do 446-701, Korea. 2.—Department of Biomedical Engineering, Carnegie Mellon University, Pittsburgh, PA 15213, USA. 3.—e-mail: cnkim@khu.ac.kr

There has recently been much progress in the development of materials with higher thermoelectric performance, leading to the design of thermoelectric devices for generation of electricity and for heating or cooling. Local heating can be achieved by current flow through an electric resistance, and local heating and cooling can be performed by Peltier heating and cooling. In this study, we developed computer software that can be used to predict the Seebeck and Peltier effects for thermoelectric devices. The temperature, electric potential, heat flow, electric current, and coefficient of performance were determined, with the objective of investigating the Peltier effect in a thermoelectric device. In addition to Peltier heating and cooling, Joule and Thomson heating were quantitatively evaluated for the thermoelectric device.

Key words: Numerical method, thermoelectric cooler, Seebeck effect, Peltier effect, coefficient of performance

INTRODUCTION

With the development of higher-performance thermoelectric materials, the design of thermoelectric modules has been studied with the purpose of optimization. When electric current passes through the interface between two different materials with different Seebeck coefficients, Peltier heating or cooling is observed at the interface. Because Peltier cooling is achieved without a refrigeration cycle, it can be effectively used when space for cooling facilities is limited, although the coefficient of performance (COP), defined below, is not very high.

$$\mathrm{COP} = (\text{Peltier cooling})/(\text{Applied electric power}). \quad (1)$$

There have been numerous studies of thermoelectric cooling. Goldsmid[1] predicted that thermoelectric cooling devices constructed from thermoelectric materials with ZT = 0.95 would be commercially competitive. Lofy and Bell[2] argued that, by suitable heat-transfer control, it is possible to increase the performance of thermoelectric coolers (TEC). Hou et al.[3] studied optimization of thermoelectric cooling elements with micro-scale dimensions for hotspot cooling application. Semenyuk and Dekhtriaruk[4] performed an experimental study of a cooling system based on a thermoelectric module designed for cooling light-emitting diodes. Semenyuk[5] examined the use of thermoelectric cooling for electro-optic components, and achieved optimum integration of thermoelectric coolers into an electro-optic device.

In the same way as for thermoelectric modeling studies, Hogan and Shih[6] performed a modeling study on power-generation modules based on bulk materials. Chen et al.,[7] by use of the commercial software SPICE, performed one-dimensional numerical simulation of a thermoelectric generator containing materials with temperature-dependent properties. Lazard[8] examined the nature of heat transfer in a thermoelectric device both analytically and numerically by use of FlexPde software. Shimizu et al.[9] discussed the possibility of increasing the performance of the flexible thermoelectric devices, and examined the effect on output voltage

(Received January 20, 2015; accepted May 8, 2015; published online May 21, 2015)

of the thermal conductivity of the materials used in the device, by use of the finite element method. Chen et al.[10] performed an analysis of heat transfer and current in a thermoelectric generator by use of Fluent software.

As indicated above, a variety of studies have been conducted on thermoelectric cooling and modeling. However, this work hardly discussed the nature of Joule heating, Peltier heating and/or cooling, and Thomson heating, which are basic characteristics of a thermoelectric device. In this study we developed computer software which can solve the system of energy equations, Ohm's law, and electric-charge conservation for a two-dimensional TEC with one n-leg and one p-leg, on the basis of the finite volume method. Temperature, electric potential, heat flow, and electric current, and the characteristics of Joule heating, Peltier heating and cooling, and Thomson heating of the TEC were analyzed for different ratios of the cross-sectional areas of the n and p-legs, and for different values of the input voltage difference, together with prediction of COP.

PROBLEM FORMULATION AND METHOD OF SOLUTION

Geometry and Properties

A π-type TEC has an n-leg and a p-leg, a top end plate, and two bottom end plates, as shown in Fig. 1. The properties of the n-leg and p-leg were adopted from the example module described in Refs.6 and 11. The fact that the properties are strong functions of the temperature helps us to interpret the numerical results.

For the n-leg:

$$\sigma_n = 10^7/T(\mathrm{S/m}), \tag{2}$$

$$\alpha_n = (0.2T - 400) \times 10^{-6}(\mathrm{V/K}), \tag{3}$$

$$k_n = 3/T \times 10^2(\mathrm{W/mK}), \tag{4}$$

For the p-leg:

$$\sigma_p = T \times 10^2(\mathrm{S/m}), \tag{5}$$

$$\alpha_n = 200 \times 10^{-6}(\mathrm{V/K}), \tag{6}$$

$$k_p = 10/T \times 10^2(\mathrm{W/mK}), \tag{7}$$

where σ, α, and k are the electric conductivity, Seebeck coefficient, and thermal conductivity, respectively, and n and p are subscripts for n-leg and p-leg, respectively.

The end plates, made of copper, have the following properties:

$$\sigma = 5.6 \times 10^7(\mathrm{S/m}), \tag{8}$$

$$k = 380(\mathrm{W/(mK)}). \tag{9}$$

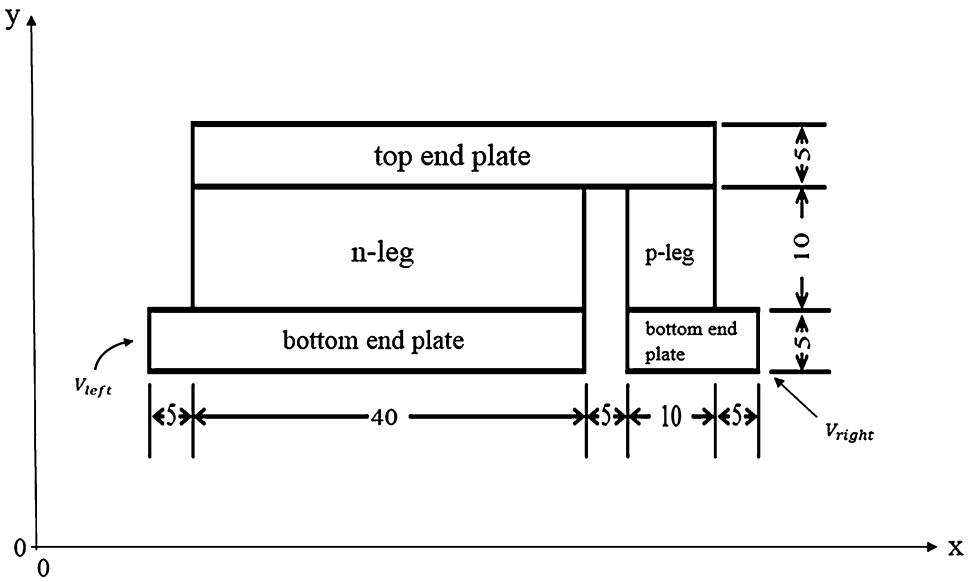

Fig. 1. Geometry and coordinate system for a typical TEC (units: mm).

Because the thermal and electric conductivity of the n-leg are smaller than those of the p-leg, the cross-sectional area of the n-leg must be increased for better performance. The dimensions of a typical TEC are given in Fig. 1; the size of the TEC in the third dimension is 10 mm.

Governing Equations and Boundary Conditions

The governing equations for temperature, electric potential, and current flow are:

Energy equation:

$$\nabla \cdot (k\nabla T) + \vec{J}^2/\sigma - T\vec{J} \cdot \nabla\alpha = 0 \tag{10}$$

with $\nabla\alpha = \frac{d\alpha}{dT}\nabla T + \nabla\alpha\Big|_{\text{interface}}$.

Ohm's law:

$$\vec{J} = \sigma(-\nabla V - \alpha\nabla T). \tag{11}$$

Conservation of charge:

$$\nabla \cdot \vec{J} = 0, \tag{12}$$

where T, $\vec{J}$, and V are the temperature, electric-current vector, and electric potential, respectively. Also, $\vec{J}^2/\sigma$, $-T\vec{J} \cdot \left(\frac{d\alpha}{dT}\nabla T\right)$, $-T\vec{J} \cdot \nabla\alpha\Big|_{\text{interface}}$ imply Joule heating, Thomson heating, and Peltier heating and/or cooling, respectively. T = 500 (K) and T = 400 (K) are the temperatures at the top side of the top end plate and at the bottom side of the bottom end plate, respectively. At the other boundaries of the computational domain, thermal insulation is assumed. Also, V_{left} = 0.0 V and V_{right} = 0.3 V are applied to the left side of the left bottom end plate and to the right side of the right bottom end plate, respectively. At the other boundaries of the computational domain, electrical insulation is assumed. The finite volume method (FVM) was used to transform the governing equations into algebraic equations, which were solved by use of the point-successive over-relaxation (SOR) method. This numerical calculation uses systems of 80 × 50–440 × 100 grids.

Typical values of the Seebeck coefficient of the n-leg, -310×10^{-6} V/K, and the p-leg, 200×10^{6} V/K, can yield the voltage difference created by the temperature difference 100 K (= 500 K − 400 K):

$$\Delta V \cong \left(-310 \times 10^{-6}\right) \times (100) = -0.031(\text{V}) \text{ for } n\text{-leg}, \tag{13}$$

$$\Delta V \cong \left(200 \times 10^{-6}\right) \times (100) = -0.031(\text{V}) \text{ for } p\text{-leg}. \tag{14}$$

Therefore, the total voltage difference for the given module is:

$$|-0.031(\text{V})| + |0.020(\text{V})| = 0.051(\text{V}). \tag{15}$$

Because the voltage difference (0.1–0.7 V) that will be discussed in the "Result and Discussion" section is larger than that (0.051 V) created by the Seebeck effect associated with the applied temperatures at the boundaries, this situation is for thermoelectric Peltier heating and/or cooling.

On the basis of these considerations, the magnitudes of Joule heating, Peltier heating/cooling, Thomson heating, and COP were obtained numerically.

RESULT AND DISCUSSION

Temperature, electric potential, heat flux, current density, Joule and Thomson heating, Peltier heating and/or cooling, and COP were addressed for a TEC with an area ratio, A_n/A_p, of 4.0 (where A_n and A_p denote the cross-sectional areas of the n-type and p-type materials, respectively) and an input voltage difference of 0.3 V. The effect of A_n/A_p on performance will be discussed, as also will the COP for a variety of input voltage differences and an A_n/A_p of 3.0.

Figure 2 shows the thermal nature of the TEC. It is apparent from Fig. 2a that regions with a temperature higher than T = 500 K are observed; this is because of Peltier heating at the interface of the top end plate with each of the n and p-legs (see also Fig. 5). Because the thermal conductivity of an n-leg (approx. 0.6–0.75 W/mK, from Eq. 4) is smaller than that of a p-leg (approx. 2–2.5 W/mK, from Eq. 7), the temperature of n-legs is usually higher than that of p-legs, in addition to the heat generated by Peltier heating. (It should be noted that the Seebeck coefficient corresponding to the highest temperature (~540 K) in the n-leg is approx. -292×10^{-6} V/K.) Because the thermal conductivity of the copper is fairly high, the temperatures of the top and bottom end plates do not vary substantially.

Heat flux is shown in Fig. 1b, where the boundary for heat flow (that is, the position of the highest temperature) is located below the interfaces of the top end plate with the n and p-legs. The heat flux in the region above this is moving upward; that below is moving downward. Close inspection reveals discontinuities of the heat flux at the interfaces of the top end plate with the n and p-legs, so the intensity of the heat flux above the interface is higher than that below the interface, because of Peltier heating. Discontinuities of the heat flux are also observed at the interfaces of the bottom end plate with the n and p-legs, because of Peltier cooling (see also Fig. 5).

The electrical nature of the TEC is depicted in Fig. 3. The distribution of electric potential is shown

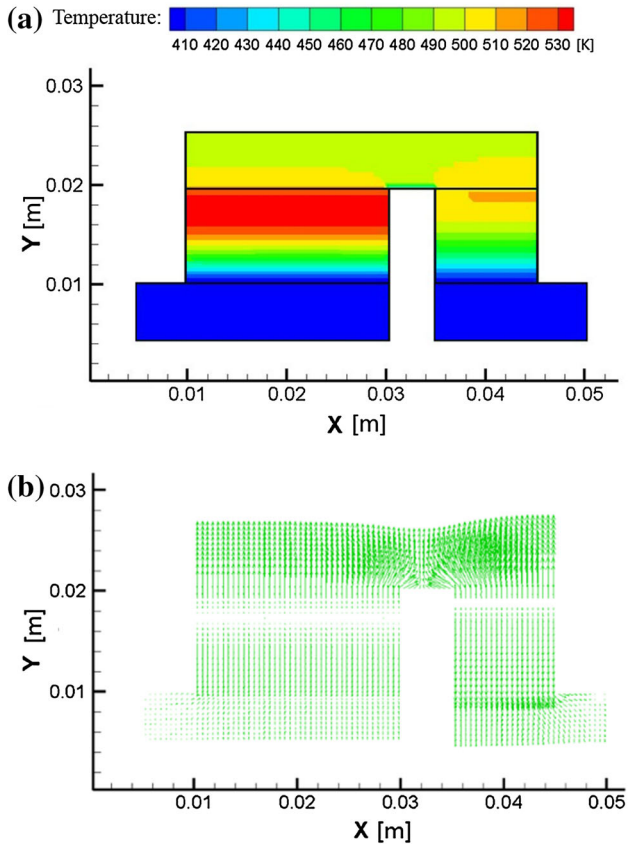

Fig. 2. (a) Temperature. (b) Heat flux.

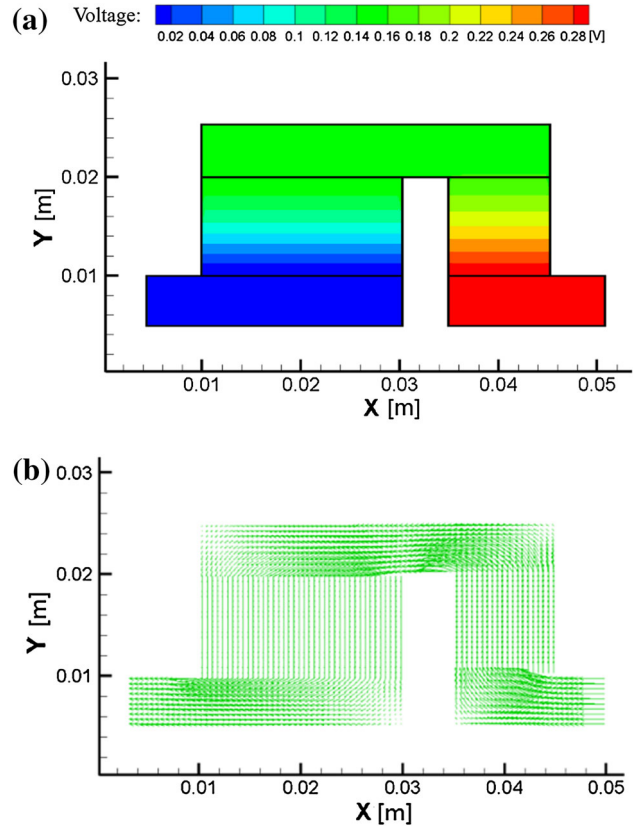

Fig. 3. (a) Electric potential. (b) Electric current.

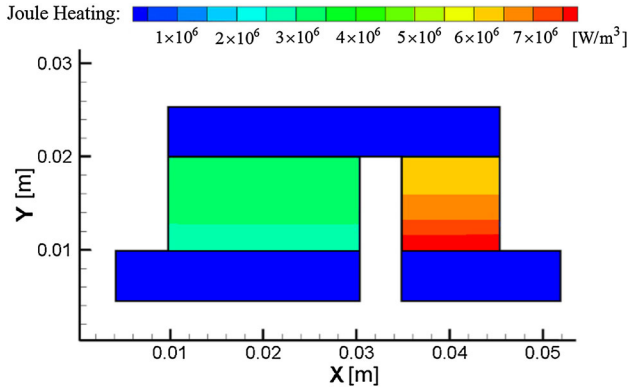

Fig. 4. Joule heating.

in Fig. 3a, where the spatial change of the electric potential in the n and p-legs is notable because the electric conductivities of the legs are smaller than those of the top and bottom end plates, and the electric potential of the top and bottom end plates is almost uniform. Figure 3b shows the detailed distribution of electric current in the device.

Joule heating is depicted in Fig. 4, in which heat generation in the n-leg is smaller than that in the p-leg, because the current density in the n-leg (with a larger cross-sectional area) is smaller than that in the p-leg, which overcomes the effect of the smaller electric conductivity of the n-leg (approx. 2.0–2.5 $\times$ 10^4 S/m, from Eq. 2) than that of the p-leg (approx. 4.0–5.0 $\times$ 10^4 S/m, from Eq. 5). Near the top interface of the p-leg the temperature is near 500 K, because of higher thermal conductivity of the top end plate and the temperature (500 K) of the top side of the top end plate. Therefore, the electric conductivity near the top end of the p-leg is approximately 50,000 S/m whereas that near the bottom end of the p-leg is approximately 40,000 S/m, with a nearly linear change in the electric conductivity in the direction of the current flow. This results in greater Joule heating in the lower part of the p-leg.

Peltier heating and cooling are depicted in Fig. 5. At the upper interfaces (i.e., the interfaces between the top end plate and the n and p-legs) Peltier heating is observed whereas at the lower interfaces (i.e., the interfaces between the bottom end plate and the n and p-legs) Peltier cooling is observed.

If the coordinate system shown in Fig. 1 is used, then the sign of the Peltier heating or cooling term $-T\vec{J}\cdot\nabla\alpha\big|_{\text{interface}}$ (and that of Thomson heating term) can be easily identified. At the lower interface of the n-leg $\vec{J}$ is downward, and α is decreasing when we move from the bottom end plate to the n-leg (across the lower interface), so that

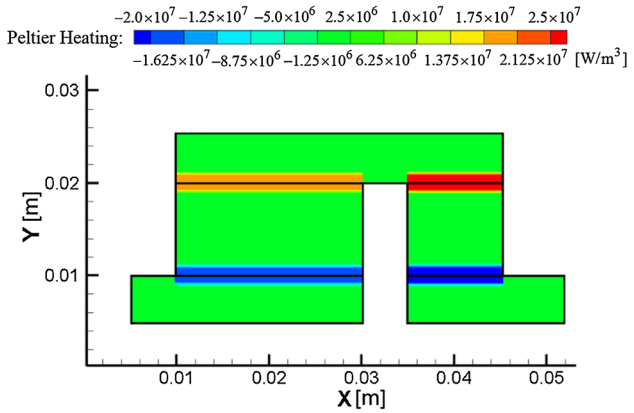

Fig. 5. Peltier heating and cooling.

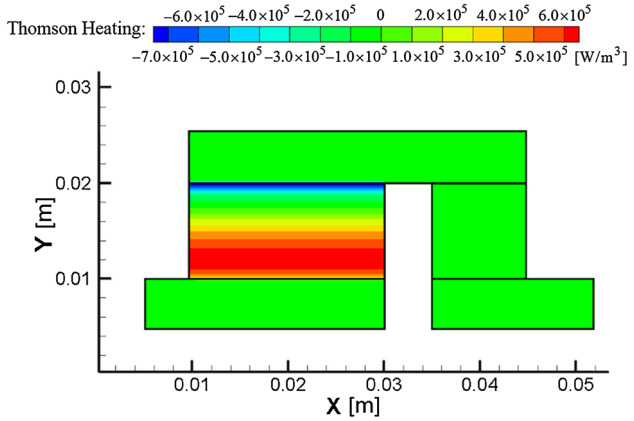

Fig. 6. Thomson heating.

$-\vec{J}\cdot\nabla\alpha\big|_{\text{interface}}$ has a negative sign, leading to cooling. However, at the upper interface of the n-leg, $\vec{J}$ is still downward, and α is increasing when we move from the n-leg to the top end plate (across the upper interface), so that $-\vec{J}\cdot\nabla\alpha\big|_{\text{interface}}$ has a positive sign, leading to heating. This consideration of the sign of the Peltier heating and cooling terms is in agreement with the depiction of Peltier heating and cooling in Fig. 5. The situation for the n-leg can be deduced similarly. The amounts of Peltier heating or cooling at the interfaces with the p-leg are usually greater than those at the interfaces with the n-leg, because the current density in the p-leg (with a smaller cross-sectional area) is higher than that in the n-leg, and this overcomes the effect of the different absolute values of the Seebeck coefficients—that between the p-leg and the top and bottom end plates (approx. 300–320 $\times$ 10^{-6} V/K, from Eq. 3) is larger than that between the n-leg and the top and bottom end plates (200 $\times$ 10^{-6} V/K, from Eq. 6).

Thomson heating and cooling is shown in Fig. 6, in which the Seebeck coefficient of the n-leg is temperature-dependent, resulting in local heating

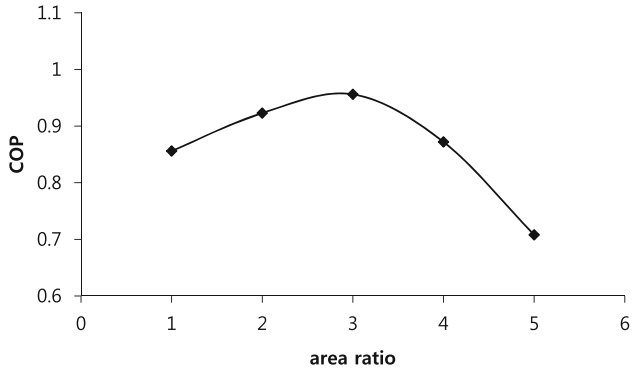

Fig. 7. COP as a function of area ratio, A_n/A_p, for a voltage difference of 0.3 V.

or cooling, whereas that of the p-leg is constant (i.e., temperature-independent) as given by Eq. 3, resulting in zero Thomson heating or cooling.

In the n-leg, the current is downward, so $\vec{J}$ has a negative value and $\mathrm{d}\alpha/\mathrm{d}T$ is positive (Eq. 3). As already discussed, the region at the highest temperature is located below the upper interfaces of the n and p-legs (Fig. 2b). This means that in the region between the upper interface and the region of highest temperature the heat flow is upward, which means that ∇T is negative. In this region, therefore, the Thomson heating has a negative value. Between the region with the highest temperature and the lower interface the heat flows downward, which indicates that ∇T is positive. This consideration of the signs of the terms matches the notation in Fig. 6.

From these figures it is apparent that the magnitudes of Peltier heating or cooling, Joule heating, and Thomson heating are approximately 10^7, 10^6, and 10^5 W/m^3, respectively. It can be valuable to consider the ratio of the magnitude of Thomson heating to that of Joule heating. On the basis of the terms in Eq. 10, this ratio can be expressed by Eq. 16, assuming that the size of $\vec{J}$ can be evaluated to be $\sigma\alpha|\nabla T|$.

$$\frac{(\text{Thomson heating})}{(\text{Joule heating})} = \frac{\left|\vec{J}\right|T(d\alpha/dT)|\nabla T|}{\left|\vec{J}\right|\alpha|\nabla T|} \approx \frac{T(\mathrm{d}\alpha/\mathrm{d}T)}{\alpha} = \frac{\mathrm{d}\alpha/\mathrm{d}T}{\alpha/T}, \tag{16}$$

where $\mathrm{d}\alpha/\mathrm{d}T$ is the dependence of the Seebeck coefficient on temperature, a property of thermoelectric materials, and T is a typical temperature of a module.

This shows that if the size of $\mathrm{d}\alpha/\mathrm{d}T$ is smaller than that of α/T, Thomson heating is negligible compared with Joule heating. In this study, the above ratio for the n-leg was evaluated to be:

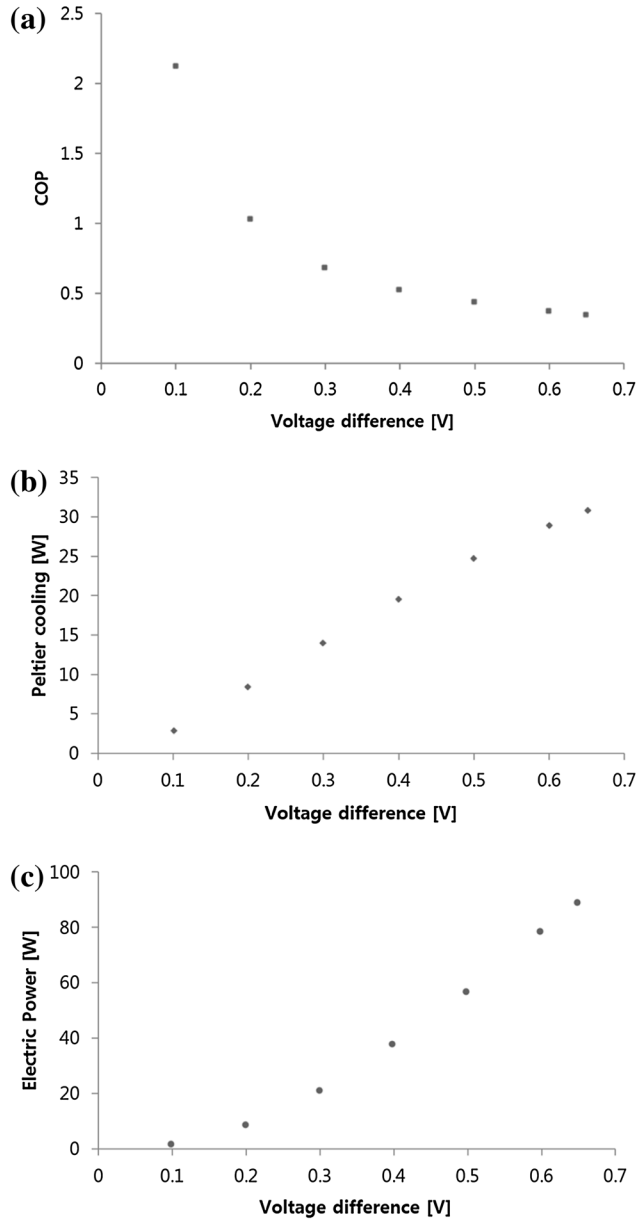

Fig. 8. Performance curves for a TEC with an area ratio $A_n/A_p = 3.0$: (a) COP, (b) Peltier cooling, and (c) electric power as functions of voltage difference.

$$\frac{d\alpha/dT}{\alpha/T} = \frac{0.2 \times 10^{-6}}{(310 \times 10^{-6})/450} = \frac{(0.2)(450)}{310} = 0.290. \quad (17)$$

Figure 7 shows the effect of the area ratio A_n/A_p on the COP. It is apparent the optimum COP is obtained when the area ratio is approximately 2.9. As discussed in the section "Geometry and properties", because the thermal and electric conductivity of the n-leg are smaller than those of the p-leg, for high-performance modules the cross-sectional area of the n-leg must be larger than that of the p-leg.

Figure 8 shows performance curves for a TEC with $A_n/A_p = 3.0$. As shown in Fig. 8a, the situation considered above, i.e. a voltage difference of 0.3 V, yields a COP of 0.6843 on the basis of input electric power of 20.49 W and Peltier cooling of 14.02 W (Fig. 8b). COP decreases as the voltage difference increases.

The increase of Peltier cooling and electric power with increasing voltage difference are shown in Figs. 8b and c, respectively. For higher values of the voltage difference, the slope of the Peltier cooling plot is smaller whereas that of the electric power plot is larger. This implies that a higher voltage difference results in a lower COP, as shown in Fig. 8a.

CONCLUSIONS

In this study we numerically investigated the performance of a two-dimensional thermoelectric cooler on the basis of the finite volume method (FVM) and the point-SOR algorithm. In contrast with previous work on thermoelectricity, in this study we performed detailed analysis of Joule heating, Peltier heating and cooling, Thomson heating, and COP.

The properties of the thermoelectric materials used in this study are strong functions of the temperature, which helped us to interpret the numerical results.

The two-dimensional geometry of the thermoelectric cooler studied in this work, dispensing with a three-dimensional model, seems reasonable, in the sense that the heat flux and electric current would not change meaningfully in the third dimension.

In summary, this numerical study reveals it is possible to predict the performance of a thermoelectric cooler. This could lead to optimization of the design of thermoelectric devices.

REFERENCES

1. H.T. Goldsmid, *Electronic Refrigeration* (London: Pion Ltd, 1986).
2. J. Lofy and L.E. Bell, in *Proceedings of the 21st International Conference on Thermoelectrics*, (2002), pp. 471–476.
3. P.Y. Hou, R. Baskaran, and K.P. Bohringer, *J. Electron. Mater.* 38, 950 (2009).
4. V. Semenyuk and R. Dekhtriaruk, *J. Electron. Mater.* 42, 2227 (2013).
5. V. Semenyuk, *Thermoelectrics Handbook*, ed. D.M. Rowe (Boca Raton: Taylor and Francis, 2006), p. 58-1.
6. T.P. Hogan and T. Shih, *Thermoelectrics Handbook*, ed. D.M. Rowe (Boca Raton: Taylor and Francis, 2006), p. 12-1.
7. M. Chen, L.A. Rosendahl, T.J. Condra, and J.K. Pederson, *IEEE Trans. Energy Conv.* 24, 112 (2009).
8. M. Lazard, *in Proceedings of the 7th IASME/WSEAS International Conference on Heat Transfer, Thermal Engineering and Environment (HTE 09)* (2009), pp. 129–134.
9. K. Shimizu, Y. Takase, and M. Takeda, *J. Electron. Mater.* 38, 1371 (2009).
10. M. Chen, L.A. Rosendahl, and T. Condra, *Int. J. Heat Mass Transf.* 54, 345 (2011).
11. B. Sherman, R.R. Heikes, and R.W. Ure Jr, *J. Appl. Phys.* 31, 1 (1960).